Scientific Papers of the University of Pardubice, Series A; Faculty of Chemical Technology
27 (2021) 151–170.

UNIVERSITY OF PARDUBICE
FACULTY OF CHEMICAL TECHNOLOGY

Effect of silver addition on thermal properties of $(GeS_2)_{50}(Sb_2S_3)_{50}$ glass

Michaela Včeláková*, Petr Košťál, and Pavla Honcová

Department of Inorganic Technology,
The University of Pardubice, CZ–532 10 Pardubice, Czech Republic

Received: May 25, 2021; Accepted: June 22, 2021

Thermal properties of the $(GeS_2)_{50}(Sb_2S_3)_{50}$ glass without and with the addition of 10 at. % of silver has been studied using calorimetry and thermal analysis. The viscosity data were obtained in a wide temperature range and described by the appropriate model. The glass transition region and the crystallization behaviour were studied in detail.

Keywords: Chalcogenides; Viscosity; Thermal expansion; Glass transition

Introduction

The chalcogenide glasses are materials with interesting properties for their application. Due to their transmittance in the infrared region of the spectrum, they are often used in IR optics, such as optical fibers, filters, lenses, etc. The great advantage of these glasses is their high resistance to air humidity. Thanks to this, they have a greater potential of applicability [1]. Viscosity is a key property to prepare chalcogenide bulk samples and glass fibers, as well as to describe their long-term stability and glass/crystal phase transition [1,2].

The Ge-Sb-S glasses are widely studied due to their attractive properties and possible applications. Their importance is given by the formation of stable ternary glasses in a wide range of compositions. Ge-Sb-S chalcogenide glasses are important mainly for their use in nonlinear optics. The glass of the system $(GeS_2)_x(Sb_2S_3)_{100-x}$ is formed by tetrahedral units GeS_2 and bipyramids Sb_2S_3. By

* Corresponding author, ✉ michaela.vcelakova@student.upce.cz

using Raman spectroscopy, it is possible to find symmetric and asymmetric vibrations of $SbS_{3/2}$ units and symmetric vibrations of similar GeS_2 units [3]. There are no strong binding interactions between the structural units [4].

According to Svoboda et al. [5], Raman spectra of the Ge-Sb-S glasses can be deconvoluted into several peaks assigned to vibrations that correspond to the Sb-Sb bonds, tetrahedral units GeS_4, Sb-Sb vibrations in bipyramidal units (S_2)Sb-Sb(S_2), (SSb)Sb-Sb(S_2) or (Sb_2)Sb-Sb(SSb), Ag_2S vibrations, SbS_3 pyramidal symmetric/ asymmetric fragments, Ge-Ge bonds, edge and corner shared GeS_4 units and bridged sulphur. According to this work, added silver atoms bind preferentially to sulphur atoms originally bound to the Sb-S units, which results in isolated antimony units. Fraenkl et al. [6] proposed four possible ways of incorporating silver atoms into a glass structure. Based on the knowledge of binding the pure Ge-Sb-S system, these authors ruled out two ways of silver binding. The decisive factor for choosing the proper binding mechanism was the binding energy. This parameter for the Sb-S bond is lower than the binding energy of Ge-S. There is also an increase in hardness, probably due to the ability of silver to fill cavities inside the glass structure.

The thermokinetic behaviour of the $Ag_x[(GeS_2)_{50}(Sb_2S_3)_{50}]_{100-x}$ system was studied by Svoboda et al. [5]. They investigated the structural relaxation and crystallization of a materials containing up to 25 at. % Ag using differential scanning calorimetry (DSC) in temperature range of 100–450 °C. The relaxation behaviour was described by the TNM model and being found to be only weakly dependent on Ag doping. On the other hand, the Ag doping increased the tendency of crystallization. The results of thermokinetic study were compared with the information obtained by Raman spectroscopy and XRD.

Fraenkl et al. [6] in their work investigated the effect of silver addition on the glass structure of nine samples from $Ag_x[(GeS_2)_{50}(Sb_2S_3)_{50}]_{100-x}$ system (x = 0; 0.1; 1; 5; 7.5; 10; 12, 5; 15; 17.5; 20 and 25). These authors investigated the change in physical properties such as glass hardness, electrical properties and mobility of silver ions by impedance spectroscopy and radioactive silver diffusion monitoring. It was found that the electrical conductivity of the direct current increases exponentially for samples in composition range of 1–20 %. The hardness also increases with the increasing amount of silver.

The viscosities of materials from the pseudobinary system $(GeS_2)_x(Sb_2S_3)_{100-x}$ (x = 10–90) measured by penetration method was published by Shánělová et al. [7]. The parallel-plate method was also used for composition $(GeS_2)_{30}(Sb_2S_3)_{70}$.

The aim of this work was to study the viscosities of the prepared $Ag_x[(GeS_2)_{50}(Sb_2S_3)_{50}]_{100-x}$ (x = 0; 10) samples in a wide temperature range, followed by their characterisation by thermomechanical analyser (TMA) and differential scanning calorimeter (DSC).

Viscosity

Viscosity is one of the most important property of a glass-forming material. Thermomechanical analyser allows to measure viscosity by combination of two experimental ways – penetration and parallel-plate method, when both approaches are usually being performed under isothermal conditions. Their schematic arrangements are shown in Fig. 1.

Penetration method firstly used by Cox [8] is based on the principle of indenter penetration into the sample. The measurement is given by specifying the indentation depth (h) of the indenter at a constant force over a period of time (t). The most frequently used indenters are hemispherical and cylindrical indenters. By applying this method, it is possible to measure viscosities in the range of 10^7–10^{13} Pa s. The cylindrical indenter is conveniently used for lower viscosities from the mentioned range; typically, in the range of 10^7–10^{11} Pa s and most often in the range of 10^9–10^{13}. Compared to this, the hemispherical indenter is more appropriate for measurements of viscosity in the range of 10^9–10^{13} Pa s.

When cylindrical indenter is used the viscosity can be calculated using the following equation [9]:

$$\eta = \frac{F}{8R_r\left(\mathrm{d}h/\mathrm{d}t\right)} \tag{1}$$

where F stands for the applicated force, R_r is the diameter of the indenter, and dh/dt the penetration rate.

The equation formerly used for the hemispherical indenter was [10]:

$$\eta = \frac{9R_rFt}{16a^3} \tag{2}$$

where a stands for the radius of the indenter impression. This equation has been derived from the idea of contact of two spheres and several assumptions: the spheres are perfectly incompressible; the radius of the impression negligible compared to the radius of the indenter; indenter is a perfectly rigid ball; the fluid flow is controlled by Newton's law. The equation (2) can be transferred into contemporarily used form [7]:

$$\eta = \frac{9}{32\sqrt{2R_r}} \cdot \frac{Ft}{h^{3/2}} \tag{3}$$

The equation is affected by the correlation between R_r and h; the condition $R_r >> h$ must be fulfilled.

Parallel-plate method is based on pressing the sample between two parallel plates by constant force applied in given time. The parallel-plate method is used for determination of viscosities in the range of 10^4-10^8 Pa s. This method can be used in both, isothermal and non-isothermal regime and the viscosity can be calculated using the following equation [11,12]:

$$\eta = \frac{2\pi F d^5}{3V\,\mathrm{d}d/\mathrm{d}t(2\pi d^3 + V)} \tag{4}$$

where d stands for the thickness of the sample, V is the volume of the sample, and dd/dt the sample compression rate. The Eq. (4) is derived based on these assumptions: the sample is incompressible; Newton's law controls the flow; the sample does not fill the entire space in-between the plates during the measurement; the sample is shaped into a cylinder form.

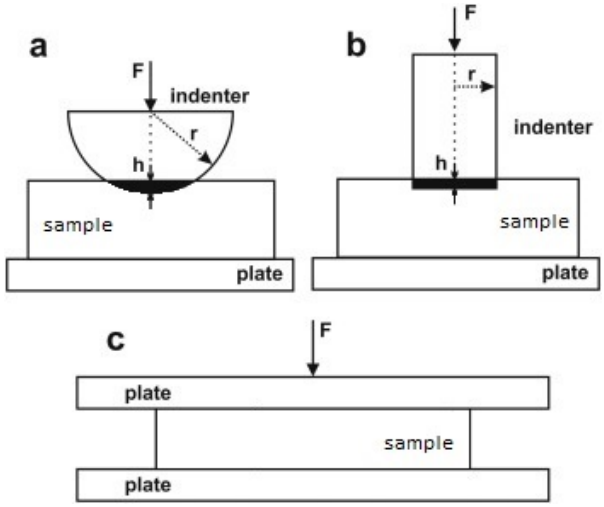

Fig. 1 Schematic arrangements of penetration (a - hemispherical, b - cylindrical indenter) method and parallel-plate methods (c)

The viscosity of glass-forming material is mainly affected by temperature change. The following equations are frequently used for description of the viscosity-to-temperature dependence of glass-formers. First of them, one has an equation of the Arrhenius type [7]:

$$\eta = \eta_0 \exp\left(\frac{E_\eta}{R\,T}\right) \tag{5}$$

here E_η stands for the apparent activation energy of the viscous flow, η_0 is the preexponential factor, R the universal gas constant (8.314 J K^{-1} mol^{-1}), and T stands for the thermodynamic temperature. The equation (5) can be rearranged into the logarithmic form:

$$\log \eta = \log \eta_0 + \frac{E_\eta}{2{,}303 R\, T} \tag{6}$$

and graphically represented by a straight line in typical viscosity-to-temperature coordinates (viscosity logarithm versus reciprocal temperature). This equation is empirical; hence, its parameters have no physical meaning. The Arrhenius type equation is used for chalcogenide glass-formers only in the narrow temperature interval.

For a wider temperature interval, the three-parameters equations are usually used. Vogel-Fulcher-Tamman (VFT) equation is one of these equations and it is commonly used in glass industry [13].

$$\log \eta = \log \eta_0 + \frac{B}{T - T_0} \tag{7}$$

where $\log \eta_0$, B and T_0 are empirical parameters of VFT equation, $\log \eta_0$ represents the viscosity at infinite temperature. This VFT equation can be also modified by other parameters (m, $\log \eta_0$, T_{12}) [14]:

$$\log \eta = \log \eta_0 + \frac{\left(12 - \log \eta_0\right)^2}{m\left(T_t / T_{12} - 1\right) + \left(12 - \log \eta_0\right)} \tag{8}$$

where m stands for steepness fragility index and T_{12} is thermodynamic temperature at which the viscosity value is equal to 10^{12} Pa s.

Another important equation is called MYEGA equation (Mauro-Yue-Ellison-Gupta-Allan) [14]:

$$\log \eta = \log \eta_0 + \frac{K}{T} \exp\left(\frac{C}{T_t}\right) \tag{9}$$

where, again, η_0 means viscosity at infinite temperature, K and C are the parameters of MYEGA equation. Also, the MYEGA equation can be modified by the same three parameters as VFT equation giving rise to the form [14]:

$$\log \eta = \log \eta_0 + \left(12 - \log \eta_0\right) \frac{T_{12}}{T_t} \exp\left[\left(\frac{m}{\left(12 - \log \eta_0\right)}\right)\left(\frac{T_{12}}{T_t} - 1\right)\right] \tag{10}$$

Yet another way of viscosity data representation is the so-called normalized Arrhenius plot or Angell plot, respectively [15]. It is the dependence of viscosity logarithm upon the reduced temperature, which is defined as the temperature of viscosity glass transition T_{12} divided by temperature. The liquids are scaled in the normalized Arrhenius diagram by the fragility parameter *m*. Two extreme cases of behaviour can be identified. (i) The parameter *m* for "strong" liquids formed by a covalent network is very low; theoretical limit being $m = 17$. The "strong" liquids can be well described by Arrhenius equation even in broad temperature interval. The typical representative of these liquids is SiO_2. (ii) The "fragile" liquids formed by a van der Walls type bonds are more susceptible to thermal degradation in the range of the glass transition. Here, the temperature dependence cannot be described by Arrhenius equation in broad temperature interval for these materials because of a strong deviation from linearity. They can be well described by VFT or MYEGA equation. An example of such a liquid is *o*-terphenyl.

Materials and methods

Glass preparation

The samples of glasses $Ag_x[(GeS_2)_{50}(Sb_2S_3)_{50}]_{100-x}$ ($x = 0$ and 10) were prepared from the pure elements (5N) by the conventional melt-quenching method. Pure elements were weighted into quartz ampoules that were evacuated to pressure approximately 10^{-3} Pa, sealed, and then put into the rocking furnace for melting and homogenization. The first step was the heating of ampoule to a temperature of 400 °C (heating rate 0.1 °C/min) and then a heating to 950 °C (heating rate 5 °C/min). The synthesis was performed at 950 °C for 20 hours and the temperature decreased down to 750 °C for 2 hours. The ampoule was quenched in cold water afterwards. The amorphous character of the prepared glasses was confirmed by X-ray diffraction.

Viscosity measurement

The viscosity was measured by two thermomechanical analysers. The first one was TMA CX03R from R.M.I (Lázně Bohdaneč, Czech Republic); the second being PT 1600 from Linseis (Selb, Germany). Before measurements, both analysers were calibrated on the melting temperature (T_m) of pure metals. For calibration was used: Ga ($T_m = 29.8$ °C), In ($T_m = 156.6$ °C), Sn ($T_m = 231.9$ °C), Pb ($T_m = 327.5$ °C), Zn ($T_m = 419.5$ °C) and Al ($T_m = 660.3$ °C). The samples for viscosity measurements were prepared in the form of plates with dimensions of approximately 6 × 6 mm and the high of 2–3 mm. The samples were ground with corundum powder.

Fig. 2 shows the example of penetration determination of viscosity by cylindrical indenter. Time dependence of the penetration depth and calculated viscosity (eq. 1) for composition with 10 at. % of silver clearly shows the equilibrating period at the beginning of the isothermal measurement. After this period, the equilibrium values of penetration rate and viscosity are reached.

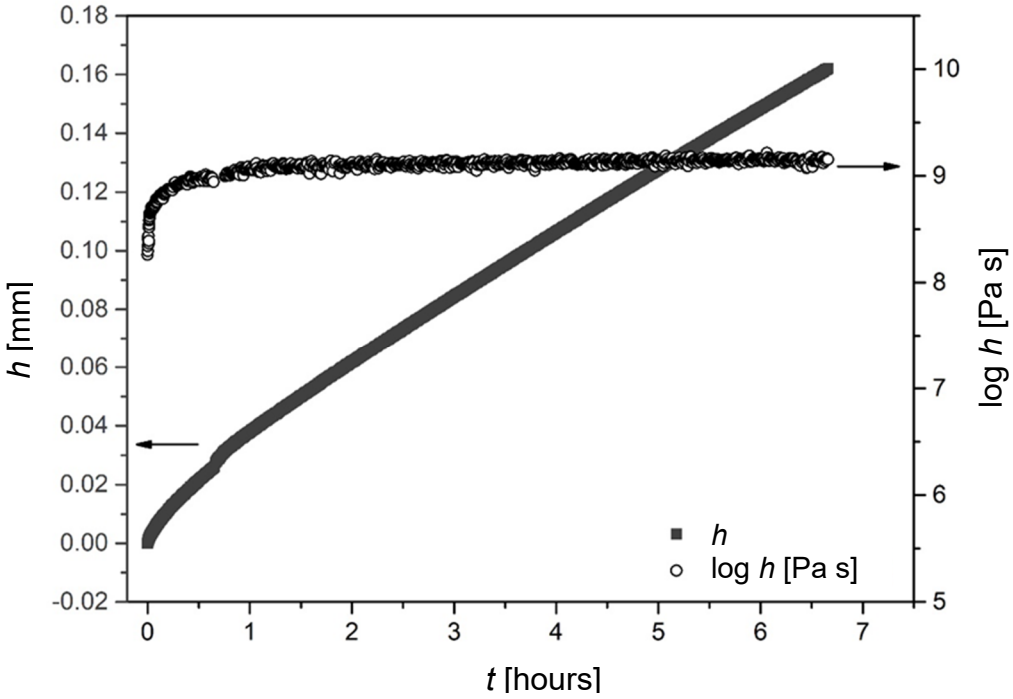

Fig. 2 Time dependencies of the penetration depth and the calculated viscosity for $Ag_{10}[(GeS_2)_{50}(Sb_2S_3)_{50}]_{90}$ undercooled melt

Glass transition temperature and thermal expansion

The measurement of the coefficient of linear thermal expansion (CTE) was performed according to the American Standard for Testing and Material (ASTM) standard [15] by TMA. According to this prescription, the CTE determination is relative, hence it has been necessary to calibrate the TMA instrument by an aluminium standard. The calibration coefficients, determined in 100 °C intervals, were calculated according to following equation:

$$k = \frac{\alpha_{\mathrm{Al,tab}}}{\alpha_{\mathrm{Al,exp}}} \tag{11}$$

where $\alpha_{\mathrm{Al,tab}}$ is standard value of CTE of aluminium, $\alpha_{\mathrm{Al,exp}}$ is experimental value of CTE. The corrected value of CTE for sample (α_{sa}) in given temperature interval is then determined by following equation:

$$\alpha_{\mathrm{sa}} = \frac{\left(\frac{\mathrm{d}l}{\mathrm{d}T}\right)^{\mathrm{sa}}}{l_0} k \tag{12}$$

where l_0 is the sample length at room temperature, $(\mathrm{d}l/\mathrm{d}T)^{\mathrm{sa}}$ is the slope of sample length dependence on temperature in given temperature interval.

Fig. 3 shows the dependence of the sample height upon temperature. When heating amorphous material below and above the glass transition region, the temperature dependence of the sample length is almost linear. The significant change in the slope of this dependence is then apparent at the glass transition temperature.

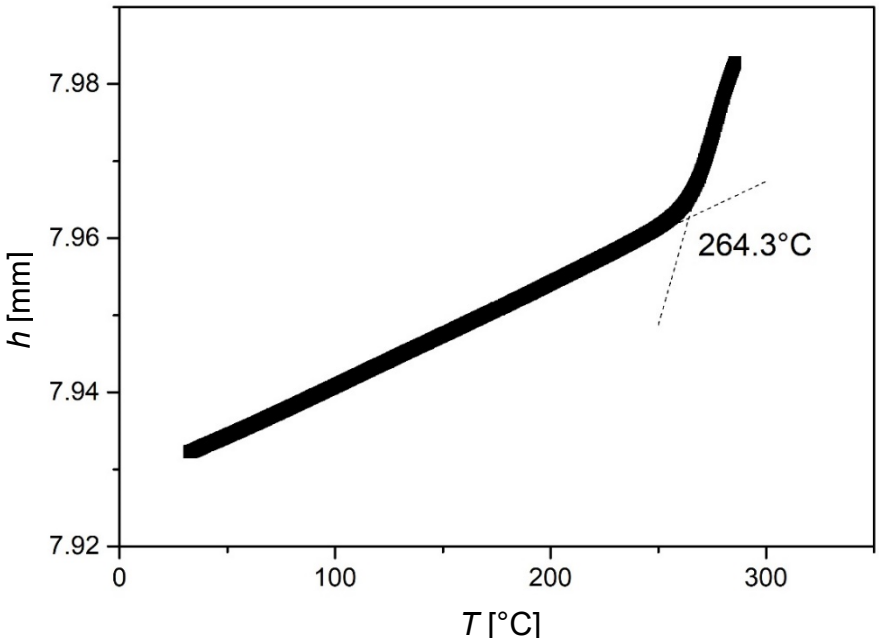

Fig. 3 Determination of the dilatometric glass transition temperature for $(GeS_2)_{50}(Sb_2S_3)_{50}$ sample (heating rate 5 °C/min)

The temperature program of CTE measurements was the same in all cases. The prepared sample was placed between two quartz plates. At the beginning of measurement, it was heated by 5 °C/min above the glass transition temperature. Subsequently, 20-min long isotherm was applied to erase the temperature history of the sample followed by its cooling with a rate of 2.5 °C/min to 40 °C to set the same thermal history before the subsequent heating measuring segment (again by 5 °C/min). This process of heating and cooling was repeated at least twice. During measuring steps, the constant force 20 mN was used; the values of the coefficients of linear thermal expansion being calculated according to equation (12).

The temperature of glass transition was measured by two methods; the first method was dilatometric measurement by TMA instrument, the second being the calorimetric measurement by Setaram DSC 131 Evo. The samples of $Ag_x[(GeS_2)_{50}(Sb_2S_3)_{50}]_{100-x}$ (x = 0; 10) were measured in standard aluminium pans. The weight of the samples was between 27 and 42 mg. Before the measurements the samples were heated by 2 °C/min above the T_g. Some 20-min long isotherm was applied above the glass transition temperature to erase of the sample history. Then the samples were cooled by 2 °C/min under the temperature of glass transition and again heated by 2 °C/min. From the curves obtained, the temperature of glass transition was evaluated as "middle point" of thermal effect associated with T_g. Every sample was measured three times.

Fig. 4 shows DSC curves for bulk samples containing 0 and 10 at. % of silver. The inset in graph illustrates the evaluation of the glass transition temperature by the midpoint evaluation.

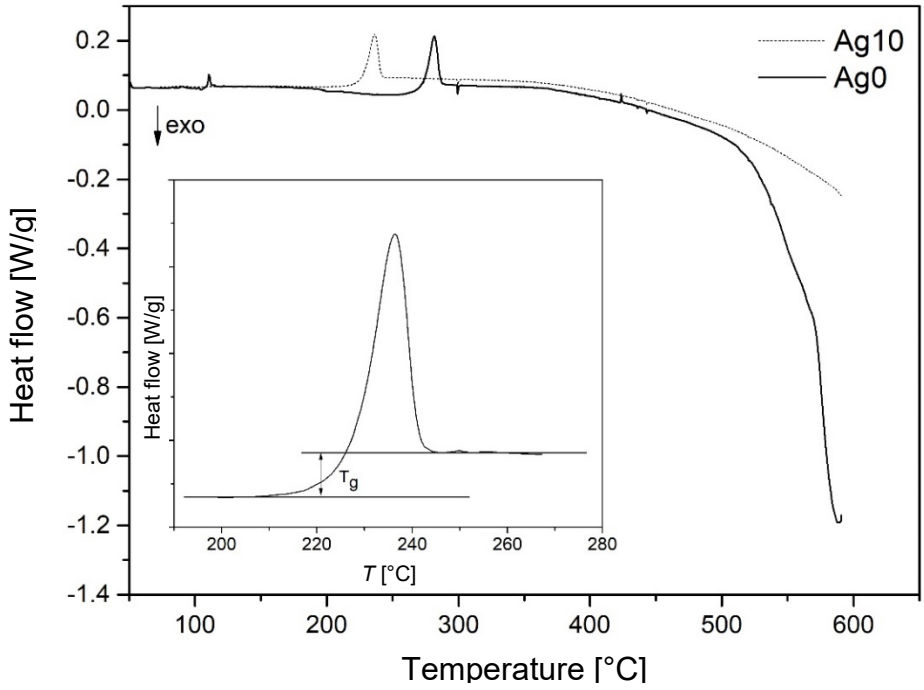

Fig. 4 DSC curves for bulk glasses with 0 and 10 at. % of Ag content (heating rate 10 K/min). Inset picture shows T_g evaluation by midpoint method for $Ag_{10}[(GeS_2)_{50}(Sb_2S_3)_{50}]_{90}$

Cold crystallization

The crystallization of the prepared samples was measured by DSC Perkin-Elmer Pyris 1 with Intercooler 2P. The DSC was calibrated by the temperature of melting of pure metals Hg (T_m = −38.83 °C), Ga (T_m = 29.8 °C), In (T_m = 156.6 °C), Sn (T_m = 231.9 °C), Pb (T_m = 327.5 °C), and Zn (T_m = 419.5 °C). The enthalpy

was calibrated by enthalpy of fusion of the pure indium. The measurements were performed using bulk samples, as well as powder form of samples, with the particle size in the range of 20–50 μm and 50–100 μm. The bulk samples of the prepared glass were crushed in an agate mortar and divided into the individual fractions using sieves.

The samples were measured in the standard aluminium pans under an atmosphere of dry nitrogen. The empty aluminium pan was then used as the reference. The sample weight was between 7 and 10 mg. The temperature range was limited by used aluminium pans and their melting temperature. Hence, the samples were heated only up to 595 °C.

Results and discussion

The temperature expansion and the glass transition temperature

The coefficients of the linear thermal expansion were determined for both compositions studied in the glass region (α_g) at 100 °C intervals and, also, estimated for the undercooled liquids (α_m) above T_g. The values for undercooled melt region are relatively inaccurate due to the starting viscous flow of the material. The specific temperature intervals in the glass region were 50–150 °C and 100–200 °C. At each interval, the dl/dT slope was determined by linear regression and the coefficient of the thermal expansion determined according to equation (12). The respective values, including their standard deviations as the precision of the measurement, are given in Table 1 and then plotted in Fig. 5.

Table 1 Coefficients of linear thermal expansion of studied samples for glass and undercooled melt regions

Chemical compounds	α_g [10^{-6}/K] 50–150 °C	α_g [10^{-6}/K] 100–200 °C	α_m [10^{-6}/K]
$(GeS_2)_{50}(Sb_2S_3)_{50}$	17.01 ± 0.29	17.02 ± 0.29	110 ± 6
$Ag_{10}[(GeS_2)_{50}(Sb_2S_3)_{50}]_{90}$	15.85 ± 0.27	16.02 ± 0.25	75 ± 4

Standard deviations, representing the precision of measurements, are also mentioned

The results show that higher values of the CTE are connected with non-doped system ($x = 0$).

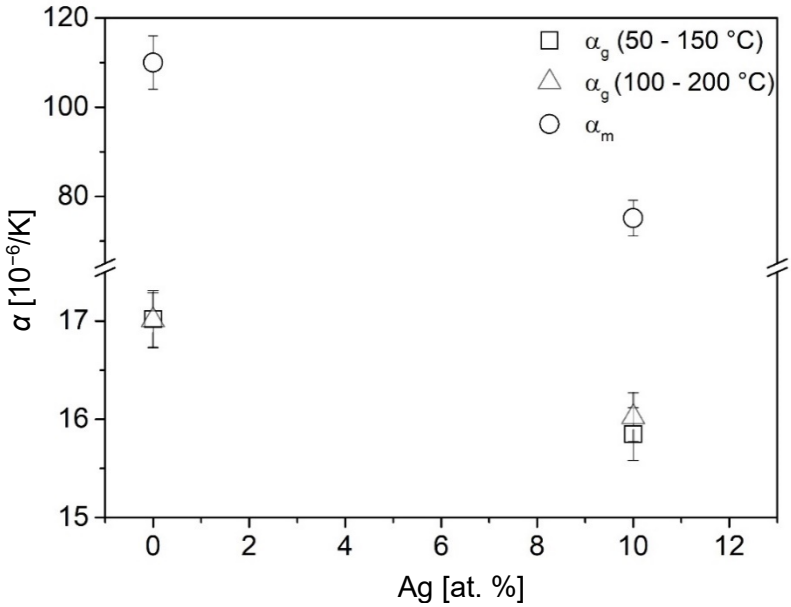

Fig. 5 Dependencies of coefficients of linear thermal expansion on the concentration of silver

The temperature of the glass transition is an important parameter for characterization of the material. The values of T_g are dependent on the heating/cooling rate, the thermal history and on the method of their determination. Therefore, the T_g value is not a material constant. The glass transition temperatures of prepared samples were determined by various methods, namely dilatometrically, by DSC, and from viscosity data. The values determined by DSC and dilatometrically applied to the point of the largest change of the measured quantity. An example of T_g dilatometric evaluation is shown in Fig. 3, DSC evaluation depicted in Fig. 4. The viscosity glass transition temperature T_{12} was determined as the temperature at which the viscosity value has reached 10^{12} Pa s. The values of the glass transition temperatures obtained for studied samples are summarised in Table 2. T_{12} values were calculated from Arrhenius fit through experimental data. It is obvious that T_g depends on the silver concentration. Fig. 6 then surveys our results together with the data published by Freankel [6] determined by DSC. The decrease of T_g values with the increasing silver content is apparent. By comparing the glass transition temperatures obtained by various methods, the lowest values were determined from the viscosity data (i.e. T_{12}). Fig. 6 also shows the standards deviations of measurements representing the precision of the T_g determination. The standards deviations are smaller than the depicted points themselves.

The T_g values published by Freankel [6] (Fig. 6) exhibit a similar trend as the values obtained in this work. However, the shift between the values is significant. This is probably caused by the higher heating rate (5 °C/min [6], in this work 2 °C/min for DSC measurements) and, also, probably by another way

of T_g. value evaluation. This presumption is supported by the data plotted in Fig. 7. Our DSC T_g values presented in Fig. 6 were determined as the so-called middle point evaluation according to ISO 11357-2. On the other hand, data presented in Fig. 7 were determined by the inflection point method. In the work of Fraenkl et al. [6], the method of T_g determination is not specified. Nevertheless, due to the similarity of the data in Fig. 7, it seems that they have determined T_g values by the inflection point method.

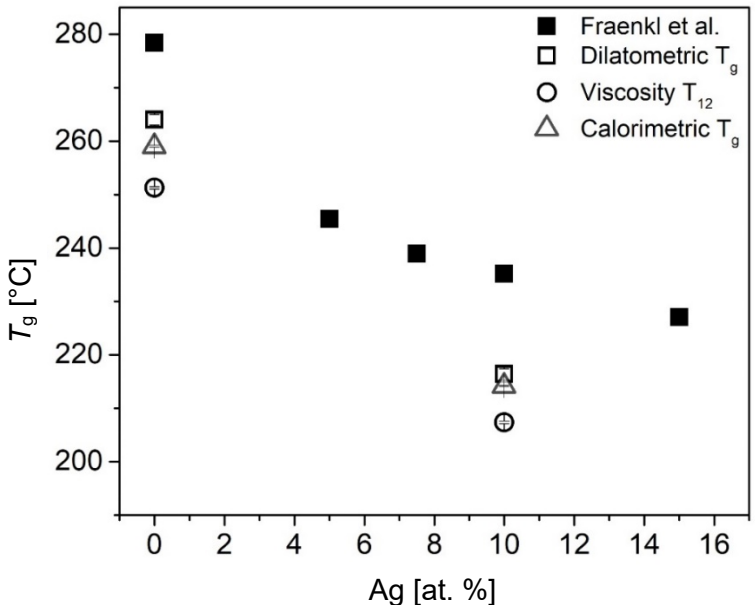

Fig. 6 The dependencies of the glass transition temperatures (middle point evaluation for DSC data) on the silver concentration compared with the values obtained by Fraenkl et al. [6]

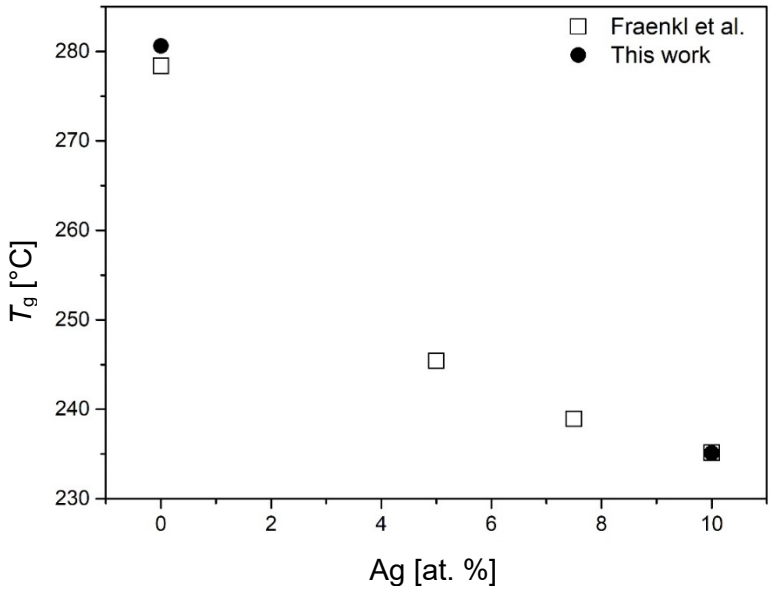

Fig. 7 Comparison of glass transition temperature values determined by DSC (inflection method, heating rate 5 °C/min) with values obtained by Fraenkel et al. [6]

Table 2 T_g values of studied samples determined by different methods

Chemical compounds	Dilatometric T_g [°C]	DSC T_g [°C]	Viscosity T_{12} [°C]
$(GeS_2)_{50}(Sb_2S_3)_{50}$	264.0 ± 1	259.0 ± 0.2	251.2 ± 0.2
$Ag_{10}[(GeS_2)_{50}(Sb_2S_3)_{50}]_{90}$	216.4 ± 1	214.1 ± 0.1	207.3 ± 0.3

Viscosity

The viscosities of glassy $Ag_x[(GeS_2)_{50}(Sb_2S_3)_{50}]_{100-x}$ (x = 0; 10) were measured by penetration and parallel-plate methods in the range of 10^6–10^{13} Pa s. The experimental data are summarized in Table 3.

Table 3 Experimental data of viscosities for compositions $Ag_x[(GeS_2)_{50}(Sb_2S_3)_{50}]_{100-x}$ (x = 0; 10) measured by: ■ penetration method with hemispherical indenter; ● penetration method with cylindrical indenter; ▲parallel-plate method

x = 0 T [°C]	CX03R log η		x = 0 T [°C]	Linseis log η		x = 10 T [°C]	CX03R log η	
252.3	11.98	■	241.7	12.80	■	201.4	12.47	■
252.7	11.88	■	246.5	12.53	■	201.7	12.65	■
267.2	10.50	■	248.7	12.14	■	207.4	12.05	■
268.9	10.43	●	252.7	11.88	■	211.1	11.68	■
271.2	10.36	●	253.5	11.92	■	215.7	11.26	■
286.8	8.97	●	259.0	11.34	■	222.6	10.57	■
304.3	7.61	●	261.2	11.02	■	230.0	9.89	●
312.3	6.89	▲	264.4	10.80	■	232.0	9.76	■
319.5	6.47	▲	265.2	10.50	■	238.2	9.14	●
			247.3	9.97	●	244.9	8.59	●
			279.4	9.62	●	251.1	8.18	●
			280.8	9.50	●	255.8	7.66	●
			285.4	9.13	●	262.7	7.16	▲
			286.8	8.97	■	269.9	6.64	▲
			293.4	8.46	●	275.0	6.22	▲
			293.4	8.45	●	280.4	5.95	▲
			293.3	8.39	●			
			296.3	8.29	●			
			299.3	8.12	●			
			301.3	7.92	●			
			301.3	7.91	●			
			307.3	7.24	▲			

According to measurement of NBS standard glass [18], the expected accuracy of viscosity measurements is ±0.05 log units and accuracy of the determination of temperature is ±0.5 °C. Experimental viscosity data are also plotted in Fig. 8. The full points are values determined by TMA CX03R (R.M.I.) and the empty points determined by PT 1600 (Linseis).

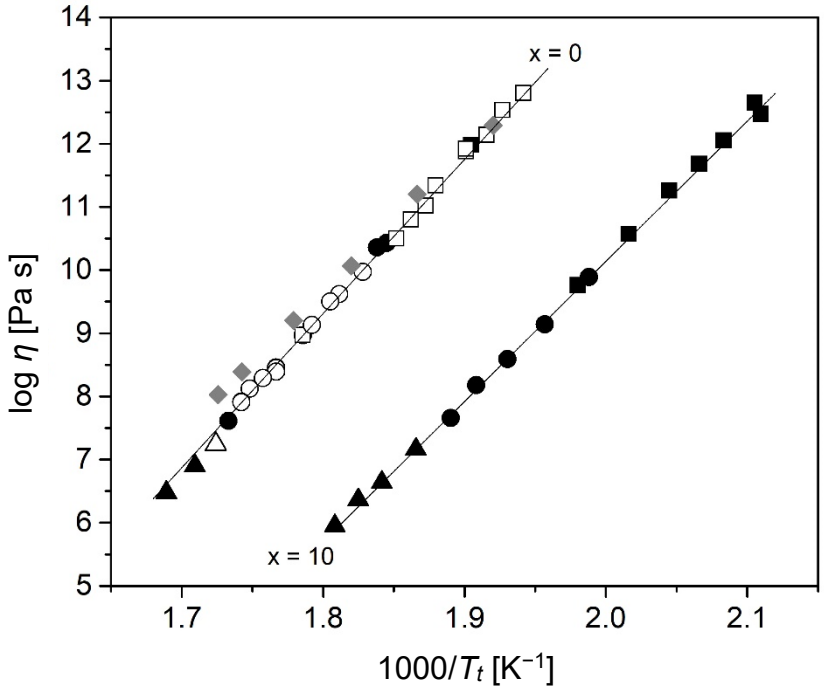

Fig. 8 The viscosities of $Ag_x[(GeS_2)_{50}(Sb_2S_3)_{50}]_{100-x}$ (x = 0; 10) determined by different methods and instruments

(■ penetration with hemispherical indenter; ● penetration with cylindrical indenter; ▲parallel-plate; full points CX03R, R.M.I; empty points Linseis)

Previously published data of Shánělová et al. [7] for $(GeS_2)_{50}(Sb_2S_3)_{50}$ are also depicted (♦)

The viscosities of non-doped system ($x = 0$) was published by Shánělová et al. (symbol ♦ in Fig. 8) [7], but only in the range of log η = 8–13 Pa·s. In this work, there is a small difference between that published viscosity values and the values determined. However, this difference is relatively common, especially for sulphur chalcogenides [17] and probably related to the relatively high volatility of sulphur and possible changes in the composition caused by it. Fig. 8 shows clearly that obtained results are not dependent on the measuring method (partially overlap of viscosities determined by penetration and parallel-plate method) and, also, on measuring instrument (identical results for both TMAs).

The linear dependencies of log η *vs*. 1000/T corresponding to Arrhenius type equation (5) were obtained for both studied compositions. The apparent activation energies of viscous flow E_η are summarized in Table 4, together with their standard deviations representing standard errors of fits.

Table 4 The values of activation energies E_η, parameters m and T_{12} determined by Arrhenius type equation and MYEGA equation (log η_0 fixed to −5) determined for studied samples

Chemical compounds	E_η [kJ/mol]	MYEGA		Arrhenius	
		m	T_{12} [°C]	m	T_{12} [°C]
$(GeS_2)_{50}(Sb_2S_3)_{50}$	484 ± 4	55.8 ± 0.7	252.4 ± 0.4	48.2 ± 0.4	251.2 ± 0.2
$Ag_{10}[(GeS_2)_{50}(Sb_2S_3)_{50}]_{90}$	429 ± 3	56.1 ± 0.7	209.4 ± 0.4	46.6 ± 0.3	207.3 ± 0.3

As mentioned above, another typical representation of viscosity data is the so-called normalized Arrhenius plot. Our data are plotted in the corresponding coordinates in Fig. 9. The fits through experimental data are also apparent in Fig. 9, representing the MYEGA fits with the fixed parameters log η_0 to value −5. This value of viscosity is expected by the normalized Arrhenius plot as theoretical value of viscosity at infinite temperature for all liquids [19]. The other two parameters of MYEGA fits (m, T_{12}) for the studied $Ag_x[(GeS_2)_{50}(Sb_2S_3)_{50}]_{100-x}$ (x = 0; 10) are shown in Table 4. These parameters can be used for prediction of viscosity in the region of melt or a region of an undercooled melt, where the cold crystallization takes place and the viscosity value are immeasurable.

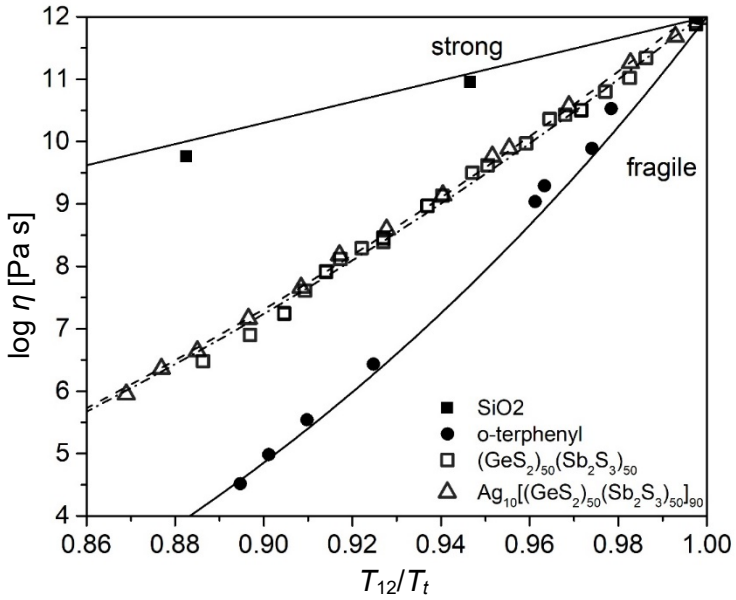

Fig. 9 The normalized Arrhenius plot depiction of experimental viscosity data determined in this work [15]

The calculated values of the steepness fragility indexes show similar values around 56 for both compositions. It seems that the fragility parameter does not significantly change with the increasing silver content.

The fragility parameter m and temperature T_{12} can also be determined from Arrhenius type equation (5). These values are also listed in Table 4, including their standard deviations representing the standards errors of fits. The values of the fragilities m determined from Arrhenius type fits show different values than those for MYEGA based fragilities. These nuances are associated with different ways of their determination (see Ref [20]). Nevertheless, both ways of fragilities determinations show the same trend – almost negligible effect of the silver content on their values.

Crystallization

The amorphous samples of the given compositions were examined by DSC. In addition to the glass transition temperature determination mentioned above, the crystallization was also studied under non-isothermal conditions. First, a higher heating rate and a bulk sample were used for both compositions. The obtained DSC curves are illustrated in Fig. 4, where the endothermic glass transition is clearly seen and followed by a gradual decrease of the signal in the exothermic direction, which corresponds to the beginning of crystallization. Unfortunately, the crystallization was not completed within the measured temperature range, which could not be increased (due to a higher limit for aluminium crucibles). Samples of both compositions after DSC measurement were studied using optical microscope and the results are illustrated in Figs. 10 and 11. Comparing the surface and the cross section of broken bulk samples, it is clear that addition of Ag into the GeS_2-Sb_2S_3 glass structure increases the crystallization – there is a very thin non-compact crystalline layer on the sample surface (see Fig. 11) in contrast to the composition without Ag (see Fig. 10).

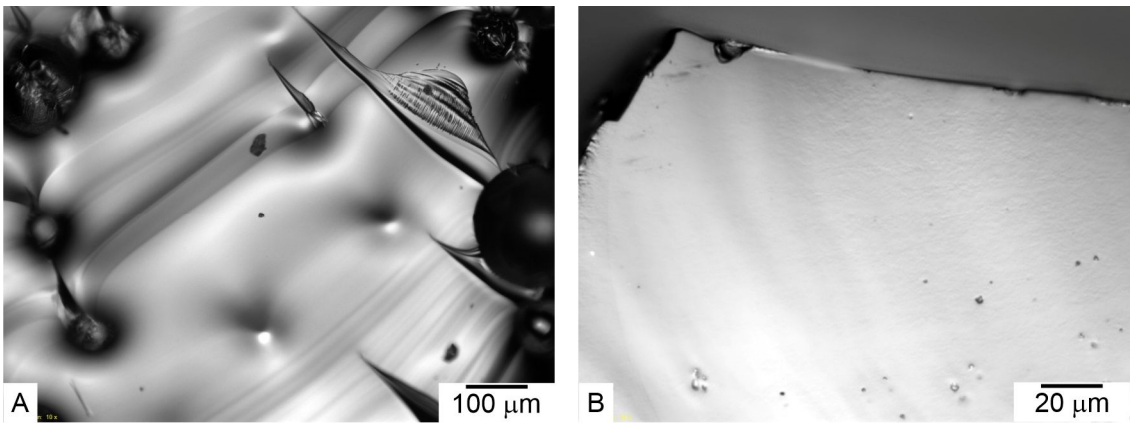

Fig. 10 Images of the $(GeS_2)_{50}(Sb_2S_3)_{50}$ bulk sample after non-isothermal DSC measurement at heating rate 10 °C/min. The surface of the sample (A) and the cross section of broken sample (B) are shown

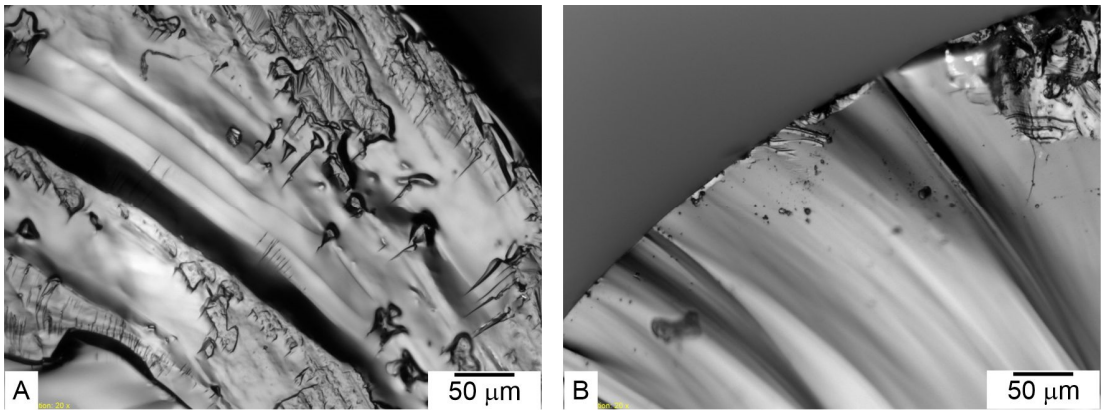

Fig. 11 Images of the $Ag_{10}[(GeS_2)_{50}(Sb_2S_3)_{50}]_{90}$ bulk sample after non-isothermal DSC measurement at heating rate 10 °C/min

The partially crystalline surface of the sample (A) and the cross section of the broken sample with a thin crystalline layer (B) are shown

Therefore, the samples were adjusted to a powder with a precisely defined particle size, which should lower the crystallization temperature in accordance with the observed surface crystallization (Figs. 10 and 11) and the results previously published by Svoboda et al. [5] for similar compositions. In addition, low heating rates were used, which also shifts the crystallization peak to lower temperatures. The illustration of the DSC curves obtained for different heating rates and particle sizes is given in Fig. 12. Unfortunately, even sample modifications did not enable to observe the entire crystallization and; therefore, no kinetic analysis could be performed. This result is not satisfactory but corresponds to the results of Svoboda et al. [5], where these authors noticed an incomplete crystallization for compositions $Ag_x[(GeS_2)_{50}(Sb_2S_3)_{50}]_{100-x}$ with x lower than 20.

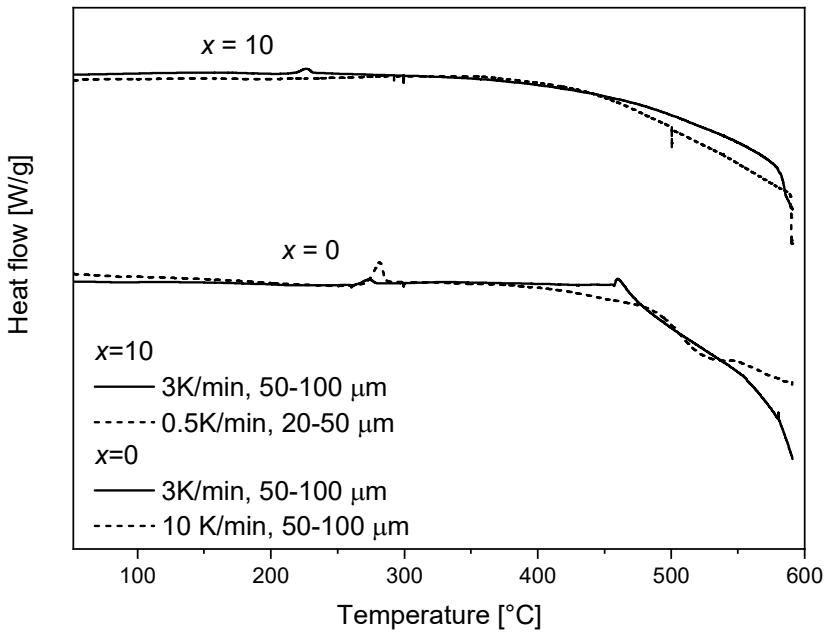

Fig. 12 DSC curves for powder $Ag_x[(GeS_2)_{50}(Sb_2S_3)_{50}]_{100-x}$ ($x = 0$; 10) samples obtained by specific heating rates

However, it is interesting that the crystallization given in Figs. 4 and 12 begins at similar temperature around 350 °C regardless of the type and composition of the sample. The effect of particle size and the Ag addition is manifesting itself in a faster decrease of the DSC signal due to the faster progress of crystallization (which is still very slow). Images from optical microscopy of the powder sample with and without Ag are given in Figs. 13 and 14. The first figure shows that the particles without Ag have some crystals on the surface, but the cross section reveals amorphous bulk of the sample. Similar results were also observed for the powder sample of composition with Ag. However, when the sample with Ag is annealed for a long time at higher temperature (Fig. 14, sample annealed at 470 °C for 800 min) we can observe more developed crystals on the surface. Nevertheless, it can be stated that although the addition of Ag into the GeS_2-Sb_2S_3 glass leads to an increase in the crystallization rate although these glasses crystallize still very slowly under the conditions studied.

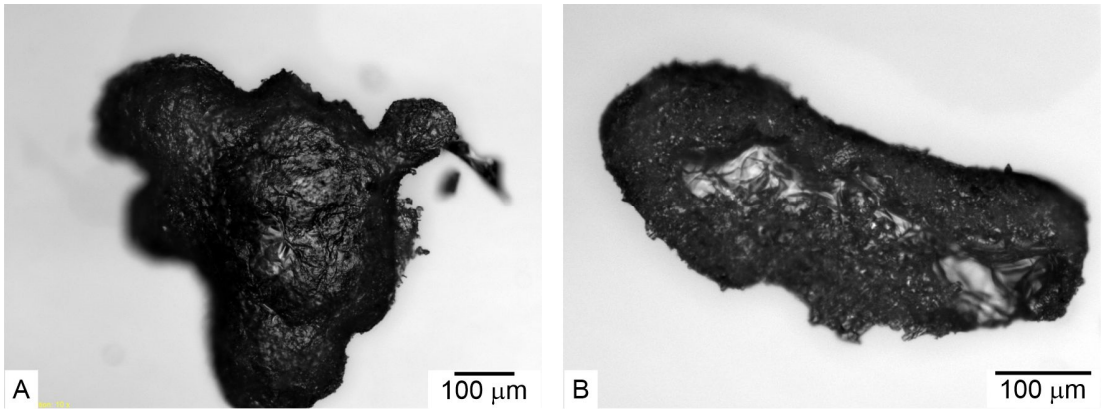

Fig. 13 Images of the $(GeS_2)_{50}(Sb_2S_3)_{50}$ powder samples (particle size of 50–100 μm) after non-isothermal DSC measurement at heating rate 3 °C/min
The surface of the particle (A) and the cross section of broken particle (B) are shown

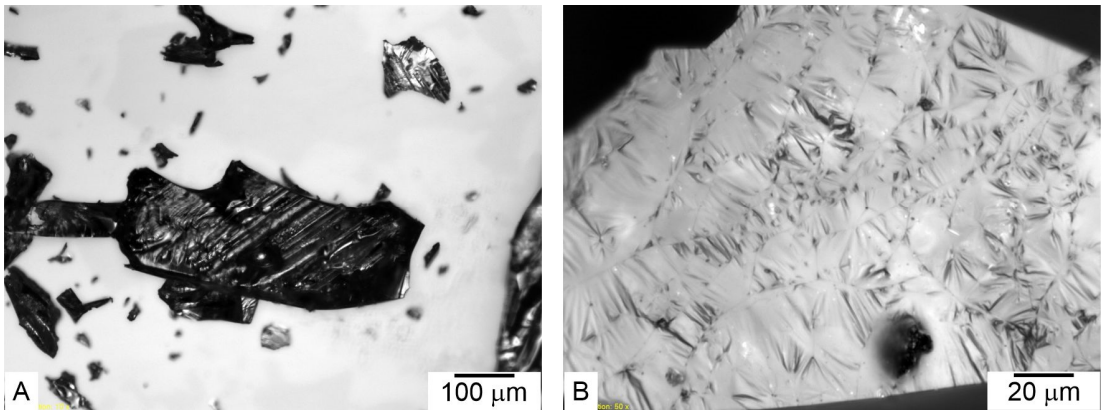

Fig. 14 Images of the $Ag_{10}[(GeS_2)_{50}(Sb_2S_3)_{50}]_{90}$ powder sample (particle size of 50–100 μm) after isothermal DSC measurement at temperature 470 °C for 800 min
The surface of particle is shown also in detail (B)

Conclusion

This work has dealt with study of the $Ag_x[(GeS_2)_{50}(Sb_2S_3)_{50}]_{100-x}$ (x = 0; 10) chalcogenide glasses. The coefficients of linear thermal expansion and the temperature dependencies of the viscosity for both studied compositions were measured by thermomechanical analyser. The viscosity data obtained by two experimental methods show a monotonic decrease of viscosity with the increasing temperature in the whole studied range of viscosities from 10^6 to 10^{13} Pa s corresponding to the Arrhenius type equation. The values of activation energy determined from Arrhenius equation are 484 and 429 kJ/mol for $(GeS_2)_{50}(Sb_2S_3)_{50}$ and $Ag_{10}[(GeS_2)_{50}(Sb_2S_3)_{50}]_{90}$, respectively. The values of the glass transition temperature exhibit a similar trend as the activation energy of viscous flow. The steepness fragility index m determined by same equation shows a similar value of about 56 for both compositions studied. The values m determined from MYEGA equation have revealed slightly different values, connected with the different way of determination, but these values are again almost independent on amount of doped silver. Both compositions (x = 0; 10) were also examined by DSC to study the crystallization of samples in the bulk and powder form. The respective DSC curves show the beginning of the crystallization process, but taking place at a relatively high temperature and remaining also uncompleted in the temperature range measured and, therefore, no kinetic analysis could be performed. Nevertheless, the obtained data show that addition of silver to the glassy structure has caused the increase of tendency to crystallization. Despite the silver added, the crystallization is a very slow process under the conditions chosen.

Acknowledgements

This work has been supported by the Internal Grand Agency of the University of Pardubice under grant no. SGS_2021_006.

References

[1] Adam J.-L., Zhang X.: *Chalcogenide glasses: Preparation, properties and applications*. Woodhead Publishing, Cambridge, 2014.

[2] Musgraves J.D., Carlie N., Hu J., Petit L., Agarwal A., Kimerling L.C., Richardson K.A.: Comparison of the optical, thermal and structural properties of Ge–Sb–S thin films deposited using thermal evaporation and pulsed laser deposition techniques. *Acta Materialia* **59** (2011) 5032–5039.

[3] Petit L., Carlie N., Adamietz F., Couzi M., Rodriguez V., Richardson K.C.: Correlation between physical, optical and structural properties of sulfide glasses in the system Ge–Sb–S. *Materials Chemistry and Physics* **97** (2006) 64–70.

[4] Lin C., Li Z., Ying L., Xu Y., Zhang P., Dai S., Xu T., Nie Q.: Network structure in GeS_2–Sb_2S_3 chalcogenide glasses: Raman spectroscopy and phase transformation study. *The Journal of Physical Chemistry C* **116** (2012) 5862–5867.

[5] Svoboda R., Fraenkl M., Frumarová B., Wágner T., Málek J.. Thermokinetic behaviour of Ag-doped $(GeS_2)_{50}(Sb_2S_3)_{50}$ glasses. *Journal of Non-Crystalline Solids* **449** (2016) 12–19.

[6] Fraenkl M., Frumarová B., Podzemná V., Slang S., Beneš L., Vlček M., Wágner T.: How silver influences the structure and physical properties of chalcogenide glass $(GeS_2)_{50}(Sb_2S_3)_{50}$. *Journal of Non-Crystalline Solids* **499** (2018) 412–419.

[7] Shánělová J., Košťál P., Málek J.: Viscosity of $(GeS_2)_x(Sb_2S_3)_{1-x}$ supercooled melts. *Journal of Non-Crystalline Solids* **352** (2006) 3952–3955.

[8] Cox S.M.: A method of viscosity measurement in the region 10^8 poises. *Journal of Scientific Instruments* **20** (1943) 113–114.

[9] Yang F., Li J.C.M.: Newtonian viscosity measured by impression test. *Journal of Non-Crystalline Solids* **212** (1997) 126–135.

[10] Douglas R.W., Armstrong W.L., Edward J.P., Hall D.: A penetration viscometer. *Glass Technology* **6** (1965) 52–55.

[11] Gent A.N.: Theory of the parallel plate viscometer. *British Journal of Applied Physics* **11** (1960) 85–87.

[12] Dienes G.J., Klemm H.F.: Theory and Application of the Parallel Plate Plastometer. *Journal of Applied Physics* **17** (1946) 458–471.

[13] Vogel H.: Das Temperatur-abhängigkeitsgesetz der Viskosität von Flüssigkeiten. Physikalishce Zeitschrift **22** (1921) 645–646.

[14] Mauro J.C., Yue Y., Ellison A.J., Gupta P.K., Allan D.C.: Viscosity of glass-forming liquids. *Proceedings of the National Academy of Sciences* **106** (2009) 19780–19784.

[15] Angell C.A.: Formation of glasses from liquids and biopolymers. *Science* **267** (1995) 1924–1935.

[16] ASTM E2113–18: *Standard test method for length change calibration of thermomechanical analyzers*, ASTM International, West Conshohocken, 2018.

[17] Košťál P., Shánělová J., Málek J.: Viscosity of chalcogenide glass-formers. *International Materials Reviews* **65** (2020) 63–101.

[18] Košťál P., Hofírek T., Málek J.: Viscosity measurement by thermomechanical analyzer. *Journal of Non-Crystalline Solids* **480** (2018) 118–122.

[19] Angell C.A.: Perspective on the glass transition. *Journal of Physics and Chemistry of Solids* **49** (1988) 863–871.

[20] Košťál P., Málek J.: Viscosity of Se–Te glass-forming system. *Pure and Applied Chemistry* **87** (2015) 239–247.